A new haptic shared controller reducing steering conflicts

Scholtens, Wietske; Barendswaard, Sarah; Pool, Daan; van Paassen, Rene; Abbink, David

DOI
10.1109/SMC.2018.00462

Publication date
2018

Document Version
Accepted author manuscript

Published in
Proceedings of the IEEE International Conference on Systems, Man, and Cybernetics (SMC 2018)

A New Haptic Shared Controller Reducing Steering Conflicts

Wietske Scholtens and Sarah Barendswaard
Dep. Cognitive Robotics
Mechanical Engineering
TU Delft
Delft, The Netherlands
{w.scholtens, s.barendswaard}@tudelft.nl

Daan M. Pool and M.M. (René) van Paassen
Dep. Control and Simulation
Aerospace Engineering
TU Delft
Delft, The Netherlands
{d.m.pool, m.m.vanpaassen}@tudelft.nl

David A. Abbink
Dep. Cognitive Robotics
Mechanical Engineering
TU Delft
Delft, The Netherlands
{d.a.abbink}@tudelft.nl

***Abstract*—When drivers have opposing intentions to a haptic shared controller which, like the driver, can continuously control the vehicle through torques on the steering wheel, the driver has to fight against the controller torque to reach their goal. This phenomenon is called haptic shared control (steering) conflicts and are a reason for drivers to reject such automation. This study is the first to realise an implementation of the novel "Four-Design-Choice-Architecture" design philosophy for shared control, hypothesized to reduce conflicts through its inherent control structure. The implemented haptic shared controller decouples reference trajectory from independent feedback and feed-forward haptic control. The implemented Four-Design-Choice haptic shared controller is compared to the baseline (predecessor) Meshed haptic shared controller through a simulator experiment. The results show that the new shared controller significantly reduces occurrence of conflicts by a factor 2.3 and significantly reduces driver torque by a factor of 3.2. Analysis shows that the novel feed-forward haptic torque and a reference trajectory supporting the drivers future (curve-entry) intentions are the dominant players in conflict reduction. The findings show that the Four-Design-Choice-Architecture is proven very effective and has large potential to further reduce conflicts with different design settings.**

***Index Terms*—Haptic Shared Control, Conflicts, Human-Machine interaction, driving simulator.**

I. Introduction

Sharing control through haptics is an alternative approach that mitigates the negative side effects that arise from traded control in highly automated vehicles [1] [2], such as loss of awareness [3] and skill degradation [4]. Haptic Shared Control (HSC) supports drivers in the steering task by providing assisting torques on an actuated steering wheel. The driver and automation jointly exert torques thereby negotiating the final steering wheel angle [5]. Several studies with different HSC implementations have shown that compared to manual driving, driving with HSC increases safety margins [6] and decreases control activity [2].

However, these improvements come at a price of increased driver torque [7], which is attributable to a misalignment of intent between driver and HSC, generally defined as a conflict. There are different ways this misalignment can take place, resulting in different types of conflicts [8], where in this study, conflict occurrence is defined as instances when the signs of torque from the driver and HSC are opposite, indicating opposing intentions. The control actions by the driver and automation must ideally complement each other, and not counteract unnecessarily. For the most HSC design philosophies, conflicts are a source of annoyance [9] [2], reducing the acceptance and thereby benefits of HSC.

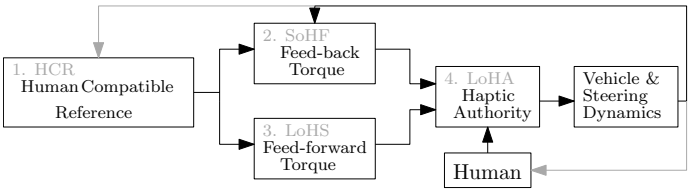

Fig. 1: The Four-Design-Choice-Architecture design philosophy from [10].

The Four-Design-Choice-Architecture design philosophy is hypothesized to reduce driver torque and increase acceptance (thereby reduce conflicts) through its inherent control structure [10]. The design philosophy is depicted in Fig. 1, the controller architecture is based on a separated Human-Compatible-Reference (HCR) trajectory, that could for example be calculated from the trajectory of a human-like driver model given current vehicle states in the sensed (previewed) environment. The essence of the control architecture following this HCR trajectory is twofold: a pure feedback component to produce compensatory torques reducing errors with the HCR (SoHF), and a pure feedforward component to produce pursuit or anticipatory torques for curve negotiation (LoHS). This decoupling of the error correction gain (SoHF) from the support for following a future trajectory (LoHS) would improve acceptance compared to only feedback [10]. These two loops are summed together contributing to the total torque. How much influence the controller has on the final angle is determined through the Level of Haptic Authority (LoHA).

A few methods have been explored to reduce conflicts including: aligning the reference with the humans trajectory (individualisation) [7] [11] or adapting the Level of Haptic Authority to grip strength [12]. However ample research has been done to investigate how a controller's structure could influence acceptance. This study is the first test the effectiveness of the inherent construct of the Four-Design-Choice-

Architecture by implementing a realisation of the architecture: the Four-Design-Choice haptic shared controller (FDC-HSC). The implementation takes an HCR that is an approximation/representation of average driver behaviour, thereby making it *compatible* with human drivers. The SoHF comprises two feedback loops on lateral position and heading, whereas LoHS feedforwards the modelled steering angle. The LoHA is set to a nominal value (only default steering wheel stiffness) meaning that authority is effectively not present.

This study evaluates the conflict reducing capabilities of the implemented FDC-HSC in a fixed-speed curve negotiation task. A two-phase simulator experiment is done where the first phase is needed to collect the empirical average driver data needed for the One-Size-Fits-All HCR. On the second phase, the FDC-HSC is compared to a baseline previously developed Meshed-HSC of [5] in terms of conflicts, subjective ratings and driver torque.

This paper starts with describing the implemented Four-Design-Choice haptic shared controller, along with the traditional Meshed controller, in Section II. After which, the experimental design, the setup of the simulator experiment, dependent variables and hypothesis are elaborated in Section III. The experimental results summarising the outcomes of conflicts, workload and subjective measures and a discussion are presented together in Section IV. Finally the main conclusions are presented in Section V.

II. Haptic Shared Control Designs

A. Four-Design-Choice (FDC) HSC

The implemented FDC-HSC, shown in Fig. 2, is an implementation of the Four-Design-Choice-Architecture (FDCA) [10], where we considered a static realisation of each of the four design choices.

1) Human Compatible Reference (HCR): As shown in Fig. 2, the FDC-HSC uses the HCR as its reference trajectory. The outputs of the *Modelled Driver Trajectory* are the coordinates of the HCR trajectory $(\vec{X}_R, \vec{Y}_R)$, the heading $\vec{\Psi}_R$ and the steering angles $\vec{\delta}_R$. The 'reference selector' block finds the index that minimizes the distance to the car's current position $(X_{car}(t), Y_{car}(t))$, the corresponding $(X_R(t), Y_R(t))$, $\Psi_R(t)$ are taken as input for the SoHF and $\delta_R(t)$ for LoHS.

In this paper the HCR was realised by offline model fitting the empirical average driver steering behaviour on a driver model that is a modification of [13]. The driver model of [13] combines feedback and feed-forward loops, assuming that driver's act upon a near angle θ_{near} that is compensated for and far angle θ_{far} that is anticipated. As opposed to [13], small angle approximations are not used in this paper, resulting in a different vehicle dynamics and body-to-global-transformation (Euler rotation matrices are used instead). The output of the model is modified to be the steering angle δ_s rather than torque T_D. Finally, an alternative way of calculating θ_{near} and θ_{far} is used, with three additional parameters being introduced: t_{far}, BSD and ESD. The near angle θ_{near} is determined as the angle the car makes to the near point: a point that is l_sm in front of the car on the road centerline. The lookahead-time t_{far} acts as a searching horizon, looking to find a tangent point, when found the far point becomes a point closely offset from the tangent point, a reachable target point [14]. When not found the far point is a point t_{LH} ahead on road center. The far angle θ_{far} is then the angle the car makes to the far point. The Begin Steer Distance (BSD) and End Steer Distance (ESD) are both threshold values that control initiation and halting of steering behaviour.

TABLE I: Haptic Shared Control parameter values used for the implemented TDCA-HSC and M-HSC

Gain	TDCA-HSC	**Gain**	M-HSC
K_s	0.05 [N]	D	0.08 [N]
K_Ψ	0.03 [Nm/deg]	P	0.9 [Nm/deg]
K_{SoHF}	1.5 [-]	K_f	2.0 [-]
K_{LoHS}	0.45 [Nm/rad]	t_{LH}	0.7 [s]

2) Strength of Haptic Feedback (SoHF): The Strength of Haptic Feedback block takes as input the HCR heading $\psi_R(t)$ and position $(X_R(t), Y_R(t))$ and compares these to the car heading $\psi_{car}(t)$ and position $(X_{car}(t), Y_{car}(t))$. The operator Δ in Fig. 2: calculates the Euclidean distance between $(X_R(t), Y_R(t))$ and $(X_{car}(t), Y_{car}(t))$. The resulting two separate feedback errors Δs_{lat} and $\Delta\Psi$, are weighted through gains K_s and K_Ψ, summed and multiplied by gain K_{SoHF} to obtain the total feedback torque T_{SoHF}. The values for the gains K_s, K_Ψ and K_{SoHF} used in this paper are given in Table I and were heuristically tuned.

3) Level of Haptic Support (LoHS): The Level of Haptic Support feed-forwards the HCR-selected $\delta_R(t)$ in an open-loop manner and multiplies this with a gain K_{LoHS} to obtain T_{LoHS}. These torques provide a distinctively different type of guidance as even if there is no deviation from the HCR trajectory you are still supported. Note the distinction between these two haptic support components, while T_{SoHF} is non-zero when there is a deviation from the reference, T_{LoHS} is independent from the car lateral or heading error, and only depends on the HCR trajectory. The gain K_{LoHS} given in Table I was heuristically tuned.

4) Level of Haptic Authority (LoHA): The LoHA determines authority the automation has over the final control output. This is done through adjusting the stiffness of the steering wheel around a particular optimal steering angle. Where a device with high authority results in a very rigid system, where the contribution of the driver is diminished. In this investigation the LoHA was set to a value of 1, meaning that the nominal steering wheel stiffness was being used with no adaptation to a particular optimal steering angle.

B. Meshed (M) HSC

The Meshed Haptic Shared Controller (M-HSC) illustrated in Fig. 3, is named as such because the strength of the generated haptic feedback is *inherently lumped* with the driver model structure that generates the trajectories. In other words, one cannot change the haptic feedback or trajectory independently from one another. This controller is triggered by the road centerline reference, selecting a road reference

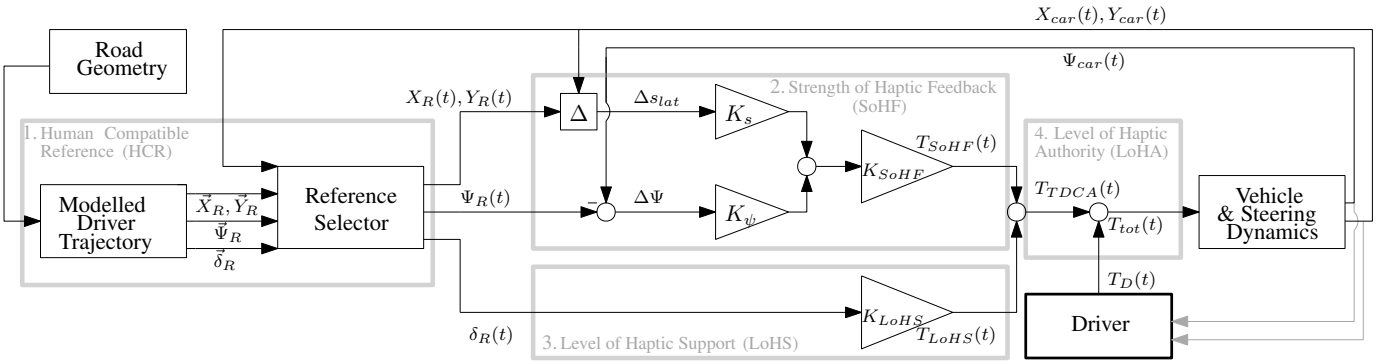

Fig. 2: The implemented Four-Design-Choice (FDC) Haptic Shared Controller derived from [10].

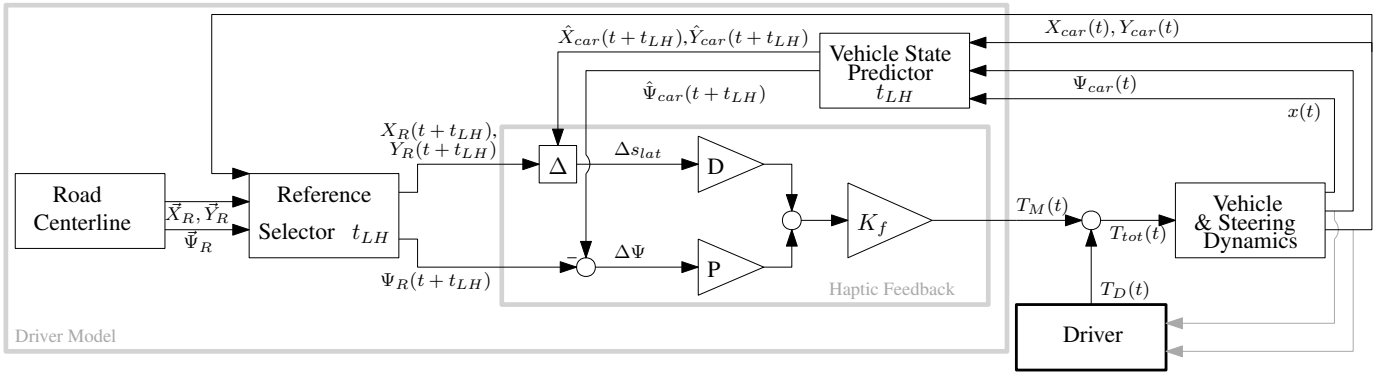

Fig. 3: The implemented Meshed (M) Haptic Shared Controller previously applied in [5]

position and heading that is t_{LH} s ahead of the closest road point to $(X_{car}(t), Y_{car}(t))$. The resulting look-ahead reference position $(X_R(t+t_{LH}), Y_R(t+t_{LH}))$ and road heading $\Psi_R(t+t_{LH})$ are then compared to the predicted vehicle states $(\hat{X}_{car}(t+t_{LH}), \hat{Y}_{car}(t+t_{LH}))$ and $\hat{\Psi}_{car}(t+t_{LH})$, respectively. The prediction is made for a constant steering wheel input with initial conditions: the bicycle model states $x(t)$, car heading $\Psi_{car}(t)$ and position $(X_{car}(t), Y_{car}(t))$, iterating the bicycle dynamics t_{LH} s ahead. Two independent feedback loops correcting for the predicted errors Δs_{lat} and $\Delta\Psi$ are weighted separately by gains D and P before being multiplied by the feedback gain K_f, to result in $T_M(t)$. The values for the gains in this controller are given in Table I and taken from [5]. Framing this controller within the FDCA framework, it is like having an HCR that is the road centerline t_{LH} s ahead, with a quickened (controlling on lookahead time t_{LH} rather than current time t) SoHF block, without any LoHS and with the same LoHA (as implemented in FDC-HSC).

III. Experiment

A. Control Task

Subjects performed a curve negotiation (lateral control) driving task in a fixed base-simulator. They were asked to drive with a fixed speed of 24 m/s on a road of width 3.6 m. Subjects negotiated five left and five right clothoidal curves with 240 m straight sections in between curves. The curve radius was 300 m with a curve length of 108 m including two clothoidal transitions of 18 m at begin and end, with a total road length of 3.7 km.

A single-track heavy sedan of 1.8 m wide was used to visually simulate the vehicle, with a vehicle dynamics identical to previous investigations [5] approximated by a bicycle model.

B. Apparatus

The driving task was performed in the fixed-based driving simulator at Human-Machine-Interface Laboratory at Delft University of Technology. The scenery was presented using three LCD projectors covering a horizontal field-of-view of 180 degrees and a vertical field-of-view of 40 degrees, with an update rate of 50Hz and an image generation delay of 10 ms.

A MOOG FCS Ecol8000S Actuator running at 2500 Hz was used for generating haptic torques on the steering wheel. Its stiffness was set to 4.2 Nm/rad over the complete deflection range; its inertia was set to 0.3 Nm/rad and the damping coefficient was 2 Nms/rad.

C. Experimental-setup and Procedure

As shown in Fig. 4, the experiment had two phases. The first phase was needed to obtain the average normal driver steering behaviour of all subjects for fitting and HCR. In the second experiment phase one independent variable was tested, namely the type of haptic shared controller, comprising three levels; the FDC HSC (**F**) , meshed HSC (**M**) and no shared control,

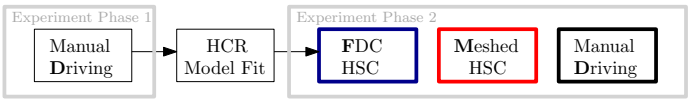

Fig. 4: Two-phase experiment design

TABLE II: Driver model parameter ranges for HCR fitting along with the right and left curve fit values.

Parameter	Range	Right Curve Fit	Left Curve Fit
K_p [-]	2:0.125:3.25	2.5	2.375
K_c [ms^{-1}]	0:1:5	4	0
BSD [m]	2.5:2.5:25	12.5	5
ESD [m]	40:5:55	55	40
t_{far} [sec]	2:0.5:3.5	3.5	3.5

unaided Driver steering behaviour (**D**). These conditions were randomised.

During both experimentation phases, the participants were given a familiarization run of 160 s before collecting data for each condition. After each run on the second day, the subjects were asked to fill out subjective ratings using a Van Der Laan acceptance questionnaire [15] to assess satisfaction and usefulness of the guidance.

D. Subjects and Instructions

The experiment was performed by sixteen subjects between the age of 23 and 28 years (average of 26.5 years), all of which have a driver's license. They were instructed to drive as they normally would and to hold their hands on the steering wheel at a "ten to two" position.

E. Fitting the HCR

To obtain a One-Size-Fits-All human-compatible reference trajectory (HCR), a driver model was fitted to the average trajectory of the sixteen drivers from the manual control trials of day 1, see Fig 5. This was done by searching for the best fit of the *lateral position* e_{lat} data, by optimising a cost function of RMSE of the average driver behaviour and a range of different modelling outputs. The range of driver modelling outputs are generated by using the road defined in Section III-A as input with a parameter range given in Table II. The parameters of the model from [13] taken as constant are: T_l = 1s, T_L = 3s, τ_p = 0.03s, K_r = 0.3, K_t= 0.5, T_N = 0.1s and l_s = 5m.

The outcome of fitting the driver model proposed in Section II-A1 is shown in the Fig. 5. The RMSE between the average driver and the HCR model fit in the lateral error domain is 0.04 m for right curves and 0.17 m for left curves. This difference is due to an average road bias of -0.1 m, where the driver's average prepositioning before curve entry was found to be 0.1m towards the outer part of the curve. Resulting in no offset for right curve entry and a -0.2m offset at left curve entry, which cannot be accounted for with the given driver model.

F. Dependent Variables

The dependent variables are given as follows:

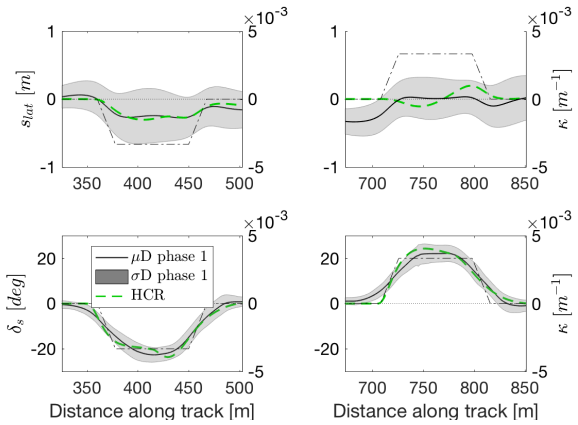

Fig. 5: Measured lateral position s_{lat} and steering angle δ_s time traces averaged over all participants during phase 1, with the curvature profile κ on the right axis

- The conflict measure in this paper is quantified by *occurrence of conflicts*, determined when the directions of the driver torque and HSC torque are opposite in direction. Depending on the direction of the driver torque, the value is either 1 or -1. For a value of 0 the HSC torque is supporting the intentions of the driver.

$$O_{conflict} = \begin{cases} 1 & \text{if } T_D \cdot T_M/T_{FDC} < 0 || T_D > 0 \\ -1 & \text{if } T_D \cdot T_M/T_{FDC} < 0 || T_D < 0 \\ 0, & \text{otherwise} \end{cases} \quad (1)$$

- The usefulness and satisfaction score from [15] was used to assess subjective acceptance.
- The workload is quantified by the driver torque applied T_D.

To evaluate the statistical significance a two-way repeated measures ANOVA was performed taking the controller type and curve direction as factors. Post hoc pairwise comparisons were also conducted. To evaluate the details of the driver's interaction with the HSCs, time traces of lateral position, steering angle, driver torque, controller torque and conflict in torques are used.

G. Hypotheses for the Experiment

There are three hypothesis for this experiment:

- H1: A decrease in occurrence of conflicts $O_{conflict}$ with the FDC-HSC compared to M-HSC.
- H2: Higher subjective usefulness and satisfaction scores from the Van Der Laan Questionnaire.
- H3: A decrease in driver torque T_D with the FDC-HSC compared to both the M-HSC and manual driving.

IV. Results and Discussion

Conflicts between human and HSC, quantified by the occurrence of conflicts $O_{conflict}$ shown in Fig. 6, shows a significant effect for HSC type (F(2,10) = 212, p<0.01) and curve direction (F(1,10) = 84, p<0.01). Moreover, there is a

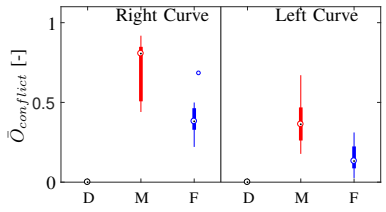

Fig. 6: Mean absolute occurrence of conflicts during curve negotiation

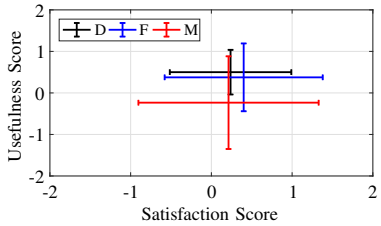

Fig. 7: Mean and STD of the Usefulness and Satisfaction score from 'Vanderlaan' questionnaire

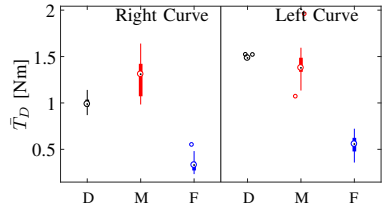

Fig. 8: Mean driver torque during curve negotiation

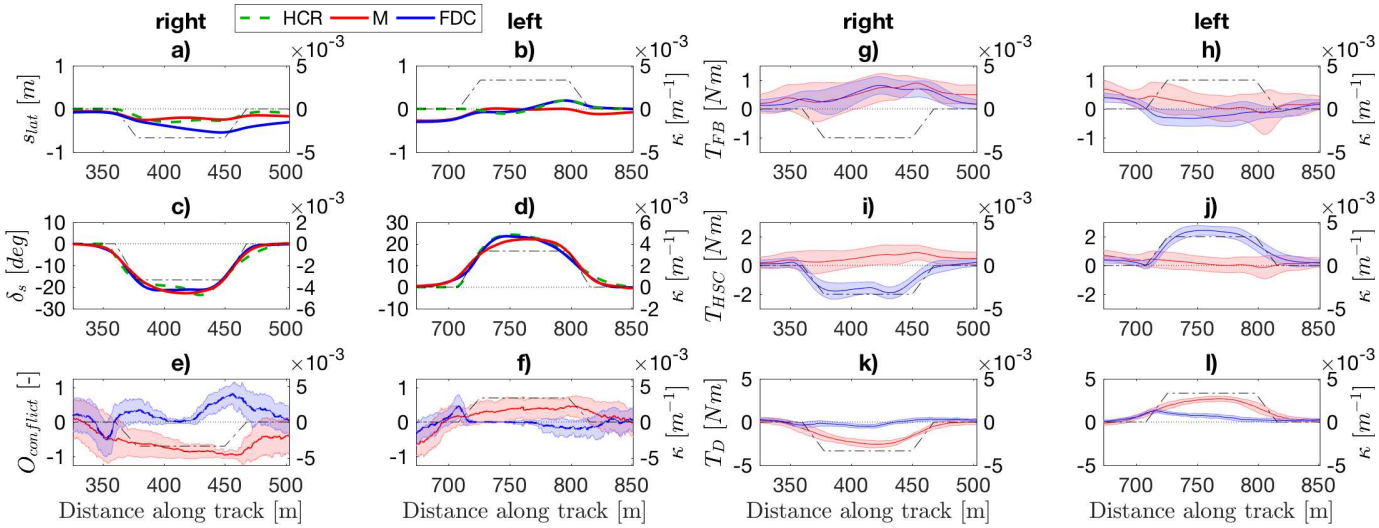

Fig. 9: Illustration of lateral position and steering angles for both left and right curves, showing the empiral average HCR and the outcomes the the driver with M-HSC and TDCA-HSC a)-d). The occurence of conflicts averaged over 5 curves, the haptic feedback torque T_{FB}, total HSC torque T_{HSC} and applied human driver torque T_D are shown for left and right curves, for the M-HSC and TDCA-HSC respectively e)-l).

significant decrease in conflicts for the FDC-HSC compared to Meshed-HSC for both right and left curves ($p<0.01$), as hypothesized (H1), with an average reduction factor of 2.3.

Figure 7 shows the subjective Usefulness and Satisfaction. The average ratings for the FDC-HSC do not significantly differ from both M-HSC and D, contrary to H2.

Driver torque T_D shown in Fig. 8, shows a significant effect for HSC type ($F(2,10) = 425$, $p<0.01$) and curve direction ($F(1,10) = 96$, $p<0.01$). Driver torque with the FDC-HSC significantly decreases for left and right curves with respect to both M-HSC ($p<0.01$) and manual driving ($p<0.01$), with average reduction factors of 3.2 and 2.8, respectively, supporting H3. To steer through a given curve a certain amount of torque is needed, the fact that driver torques were much smaller during FDC-HSC reflects not only that the FDC is contributing with feedforward torque, but also that the driver accepts this torque. Moreover, there is a significant increase in driver torque with the Meshed-HSC compared to manual driving during right curves ($p<0.01$), in line with previous findings [5].

Interestingly, the variability (standard deviation) of the occurence of conflicts is significantly larger for the M-HSC than it is for FDC-HSC ($p<0.01$). A concrete reason for this is not found yet. The significant increase in driver torque standard deviation ($p<0.01$) for M-HSC compared to FDCA-HSC is better understood and is relatable to *Motor Unit Recruitment principles*. This is clear when we understand that the amount of driver torque increases with a stronger dynamic haptic feedback [16] and that the M-HSC has larger feedback gains than FDC-HSC.

From a control-theoretic point of view, a good controller follows its reference, likewise the FDC-HSC should guide the driver to drive like its reference: the modelled average driver (HCR). However, since the driver has the capability to reject the guidance by giving opposing torques, we see that following the HCR only happens when the driver accepts the guidance. From Fig. 9a)-d) it can be seen that for the left curve the FDC-HSC follows the HCR, however this is not the case for the right curve. Consequently we see that for the right curves there are significantly more conflicts than left curves, with a moderately strong correlation between the extent to which the

FDC-HSC follows its HCR in the curve and conflicts in torque (r = 0.55).

The FDC-HSC combines feedback with feedforward (both with respect to the HCR) Fig. 2, whereas the Meshed controller consists of a haptic feedback loop (with respect to the road center t_{LH} s ahead) Fig. 3. From Fig. 9g)-j) the magnitude of feedback torque T_{FB} is very similar (especially for right curves) between both HSC. This implies that from a torque perspective, the improvement in acceptance stems from the feedforward torque. The driver's perception of these two different types of guidance in a dynamic closed loop is very different, analogous to a teacher who continuously corrects each small deviation you make (feedback), to a teacher who "shows you the way" (feedforward). This proves that the *type* of haptic shared control (Level of Haptic Support) is crucial for the acceptance of the system.

One would expect that right curves have less conflicts than left curves because the HCR is a (much) better fit for right curves, both in terms of offset and frequency behaviour. However the opposite is true: conflicts for left curves is much lower. This is evident from Fig. 9a)-d) showing that the trajectory driven with FDC-HSC for left curves is a closer match with its reference (HCR), implying agreement with the controllers motives. Conversely, for right curves the motives (HCR) are less accepted, resulting in a large adaptation of trajectory shown in Fig. 9a). This unintuitive result proves that the occurrence of conflicts is not singularly dependent on the accuracy of replicating the *exact* human driver behaviour for the HCR. It is possible that the driver was more accepting of the (unaccurate) left curve HCR triggered guidance because the left curve entry offset means that the HCR is in the direction of curve-cutting. Thereby allowing for the driver's initial intent to curve-cut at curve-entry, which builds trust, to the extent that the drivers later follow a trajectory that does not represent their (average) driver style. This allowance and agreement with the HSC is also evident from a significant decrease in absolute Feedback Torque compared to right curves, shown in Fig. 9g)-h). Again, this is not unique for the FDC-HSC, the M-HSC (having a reference of road centerline), also shows less occurrence of conflicts for left curves. Hence, as long as the (initial) direction of intention of the driver is supported, the human driver will experience less conflicts.

V. Conclusion

The goal of this study was to evaluate an implementation of the Four-Design-Choice-Architecture (FDCA) haptic shared controller: the Four-Design-Choice HSC, in terms of occurrence of opposition torques (conflicts) between human driver and controller. A human-in-the-loop simulator experiment was conducted comparing the novel FDC implementation to the previously developed Meshed haptic shared controller and no driver assistance (manual driving).

Despite the fact that the FDC-HSC did not show any significant subjective improvements, the FDC-HSC significantly reduces occurence of conflicts by a factor 2.3, and significantly reduces driver torque by a factor 3.2, compared to the Meshed-HSC. This can be attributed to two inherent design elements in the FDC-HSC; the independent feed-forward (LoHS) contribution and an HCR that supports (future) curve entry intentions. This proves that the Four-Design-Choice-Architecture is proven effective and has (larger) potential with different design choice settings.

VI. Acknowledgements

The work presented in this article was made possible by the Dutch Technology Foundation STW (VIDI project 14127), which is part of the Netherlands Organization for Scientific Research (NWO).

References

[1] F. Flemisch, J. Kelsch, C. Loper, A. Schieben, J. Schindler, and M. Heesen, "Cooperative control and active interfaces for vehicle assistance and automation," in *FISITA World Automotive Congress*, 2008.

[2] S. M. Petermeijer, D. A. Abbink, M. Mulder, and J. C. F. De Winter, "The effect of haptic support systems on driver performance : A literature survey," in *IEEE Trans. Haptics*, vol. 8, no. 4, 2015, pp. 467–479.

[3] N. Merat and A. H. Jamson, "How do drivers behave in a highly automated car?" in *Proc. Fifth Int. Driv. Symp. Hum. Factors Driv. Assessment*, 2008, pp. 514 – 521.

[4] J. C. F. De Winter and D. Dodou, "Preparing drivers for dangerous situations: A critical reflection on continuous shared control," in *IEEE Int. Conf. Syst. Man, Cybern.*, 2011, pp. 1050–1056.

[5] M. Mulder, D. Abbink, and E. Boer, "The effect of haptic guidance on curve negotiation behavior of young, experienced drivers," in *IEEE Int. Conf. on Systems, Man, and Cybernetics (SMC)*, Nov. 2008, pp. 804–809.

[6] P. G. Griffiths and R. B. Gillespie, "Sharing control between humans and automation using haptic interface: Primary and secondary task performance benefits," in *Hum. Factors J. Hum. Factors Ergon. Soc.*, vol. 47, no. 3, 2005, pp. 574–590.

[7] R. Boink, M. M. van Paassen, M. Mulder, and D. A. Abbink, "Understanding and Reducing Conflicts Between Driver and Haptic Shared Control," in *Proc. of the IEEE Int. Conf. on Systems, Man and Cybernetics, San Diego (CA)*, 2014, pp. 1510–1515.

[8] M. Itoh, F. Flemisch, and D. Abbink, "A hierarchical framework to analyze shared control conflicts between human and machine," in *Proc. of the 13th IFAC Symp. of Human-Machine Systems, Kyoto, Japan*, vol. 49, no. 19, 2016, pp. 96–101.

[9] R. Parasuraman and V. Riley, "Humans and automation: Use, misuse, disuse, abuse,," in *Hum. Factors J. Hum. Factors Ergon. Soc.*, vol. 39, no. 2, 1997, pp. 230–253.

[10] M. M. Van Paassen, R. Boink, D. A. Abbink, M. Mulder, and M. Mulder, "Four design choices for haptic shared control," *Adv. Aviat. Psychol.*, pp. 237 – 254, 2017.

[11] A. W. De Jonge, J. G. W. Wildenbeest, H. Boessenkool, and D. A. Abbink, "The effect of trial-by-trial adaptation on conflicts in haptic shared control for free-air teleoperation tasks," in *IEEE Trans. Haptics*, vol. 9, no. 1, 2016, pp. 111–110.

[12] J. Smisek, W. Mugge, J. B. J. Smeets, M. M. van Paassen, and A. Schiele1, "Adapting haptic guidance authority based on user grip," *IEEE International Conference Systems, Man, and Cybernetics*, pp. 1516 – 1521, 2014.

[13] F. Mars, L. Saleh, P. Chevrel, F. Claveau, and J. F. Lafay, "Modeling the visual and motor control of steering with an eye to shared-control automation," in *Proc. of the Human Factors and Ergonomics Society 55th Annual Meeting*, 2011, pp. 1422–1426.

[14] E. R. Boer, "Tangent point oriented curve negotiation," in *Proc. of Conf. on Intelligent Vehicles*, 1996.

[15] J. D. Van der Laan, A. Heino, and D. De Waard, "A simple procedure for the assessment of acceptance of advanced transport telematics," in *Transportation Research Part C: Emerging Technologies*, vol. 5, no. 1, 1997, pp. 1 – 10.

[16] F. Mars, M. Deroo, and J. Hoc, "Analysis of human-machine cooperation when driving with different degrees of haptic shared control," in *IEEE Transactions on Haptics*, vol. 7, no. 3, 2014, pp. 324 – 333.